DIVISION ETUDES ET DEVELOPPEMENT DES REACTEURS
Département des Réacteurs à Neutrons Rapides

Topical meeting on advances in reactor physics and shielding.
Sun Valley, Ida, USA, September 14 - 17, 1980.
CEA - CONF 5512

SYNTHESIS METHOD VALIDATION FOR SUPER-PHENIX 1 START-UP CORE STUDIES

J.Y. PIPAUD * - G. GASTALDO ** - C. GIACOMETTI

RESUME :

This paper aims at presenting the systematic studies performed in order to check and to improve the synthesis method wich is used to optimize the configuration of the SUPER-PHENIX 1 start-up core versus the diluent subassembly location and the control rod ring insertion.

A special attention is paid to the choice of the trial functions when the two rod rings have different insertion depths. Present limits of the synthesis method are given and further improvements are indicated.

* NOVATOME / PARIS
** NIRA / GENES

INTRODUCTION

1 - The enrichments of the SUPER-PHENIX I start-up core are predicted with taking into account the ± 1% ΔK/K neutronic uncertainty[1]. One has then to guarantee that, whatever will be the deviation between the predicted and real critical masses, within this ± 1% ΔK/K margin, an appropriate core loading will fulfil the reactor operation conditions during the complete length of the first cycle. In this respect three typical loadings are investigated :

- "Nominal loading", corresponding to the core where there is no deviation between the predicted and the achieved critical masses ;
- "Maximal loading", corresponding to an underprediction of the critical mass by 1% ΔK/K ;
- "Minimal loading", corresponding to an overestimation of the critical mass by 1% ΔK/K.

2 - In these three loadings the fresh core excess reactivity is compensated by replacing some of the fuel subassemblies by diluent or by inserting partially the control rod rings. For each loading the number and location of different subassemblies and the rod ring insertions are to be optimized in order to respect core operation constraints :

- limitation of the maximal linear power
- limitation of the maximal cladding temperature.

3 - This neutronic optimization requires 3D parametric calculations of the power distribution versus the diluent subassembly location and the control rod ring insertion. The synthesis method, which is particularly well suited for parametric studies, has been chosen with the following criteria :

- the synthesis method is used only to optimize the start-up configurations : for each selected configuration, the final power distribution is calculated with the 3D finite difference reference method. Therefore the following discrepancies are accepted between the synthesis method and the reference one at the level of parametric design studies :

  ± 2% on the maximum ponctual power
  ± 2% on the integrated power per subassembly (which leads to ± 4°C on the cladding temperature)
  ± 20% on the ponctual power values at core/upper axial blanket boundary (which leads to ± 3°C on the cladding temperature)
  ± 5°C on the cladding temperature.

- the synthesis flux corresponding to the selected configurations are used as "starting flux"for 3D finite difference calculations.

- the synthesis method validation is restricted to the SPx1 start-up situations in which the control rods are "in", "out" or "partially in". In the last case, the two control rod rings may be differently inserted in order to equalize the power peaks of the two core zones, the insertion depth difference being limited to ≈ 10 cm.

4 - This paper aims at presenting the studies which has been performed to calibrate and check the synthesis method for the SPx1 start-up core calculations. After a brief description of the synthesis method one checks the Galerkin's algorithm with respect to 3D finite difference calculations. Then the analysis performed in order to improve the choice of the trial functions is given, and the associated results are presented.

PRESENTATION OF THE SYNTHESIS METHOD

In the single channel synthesis method calibrated for the SPx1 design, the flux distribution is given by :

$$\phi^g(x,y,z) = \sum_{i=1}^{N} \alpha_i^g(z) \cdot \phi_i^g(x,y)$$

with using a weighted residual procedure[2]. $\phi_i^g(x,y)$ are the trial functions which correspond to plane flux distributions in different reactor slices "i" and $\alpha_i(z)$ the mixing ones. According to the Calerkin's algorithm, the weighting functions are chosen to be the same as the trial functions.

The following diagram shows the calculational procedure using the synthesis method to optimize the start-up core configurations and to provide the guess flux values for starting the final finite difference calculations

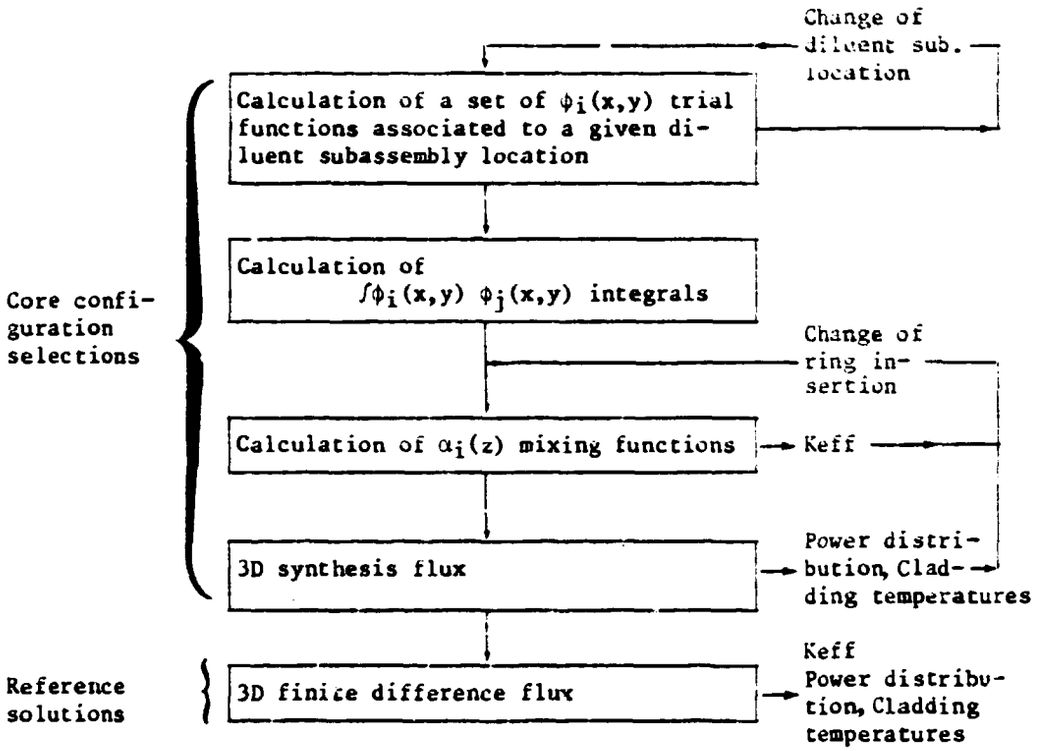

On this procedure, the following comments can be made :

- the 2D flux distribution $\phi_i(x,y)$ corresponding to the slice including the control rod followers permits a preliminary optimization of the diluent subassembly location.

- the research of the control rod ring insertions providing the desired value of Keff and equal power peaks in the two core zones does not require expensive calculations since it uses the same trial function and integral sets.

All the calculations are performed with 6-group cross sections collapsed from the 25-group CARNAVAL IV adjusted library. The trial functions are calculated in plane hexagonal geometry, with 7 mesh points per hexagon (Figure 1 gives the main geometrical characteristics of SPx1). Axially, the mesh size is ≈ 3.5 cm in the core zone.

FIRST CALIBRATION OF THE SYNTHESIS METHOD WITH "ACCURATE" TRIAL FUNCTIONS

Check of the Galerkin's algorithm

A 3D synthesis calculation using 2D trial functions extracted from the 3D finite difference flux are compared to this 3D reference calculation. The core configuration investigated is given in Figures 1 . The control rod insertion depths are : 40 cm for the inner ring (I.R) & 50 cm for the outer ring (O.R).

The trial functions involved in the synthesis calculations are plane hexagonal flux distributions corresponding to the following axial slices of the reactor :

- lower blanket
- core slice including only the control rod followers
- core slice corresponding to the ring insertion depth difference
- core slice including the absorber part of the two rings
- upper blanket.

The first column of Table I shows that when one uses the five trial functions representing the different axial reactor slices, the Galerkin's algorithm gives results quite consistent with the finite difference method.

Choice of the trial functions

Figure 3 presents typical radial 2D flux distributions extracted from the 3D finite difference calculation (corresponding to the above-mentioned trial functions). One observes that these 2D fluxes does not significantly characterize the axial reactor slices. One can classify :

- a flat shape corresponding to slices where there is no strong perturbation (lower blanket and core slice including a part of the followers) ;

- a shape including two depressions due to the absorbers (upper blanket and core slice including the two absorber rings) ;

- an "intermediary" shape corresponding to a slice located below the tips of the rods.

Taking into account that there are only two shapes which are significantly different, one is led to try to use only two trial functions for the synthesis calculations : the "follower" and "absorber" trial functions. The second column of Table I shows that the deviations of results from the reference solution are very acceptable as far as the design parameters are concerned. In Figure 2, the $\alpha_i(z)$ distributions point out the distinctive slices, especially the transition zone.

Set of two trial functions for different rod ring insertions

The above-mentioned set of two trial functions is used to construct a 3D synthesis flux corresponding to the new ring insertion depths : 40 cm (I.R) and 45 cm (O.R). The third column of Table I shows that the deviations of results from the corresponding reference solution are increasing. Explanations are given in Figure 4 which shows the high amplitude flux disturbance resulting from a differential movement of rings. The change of the insertion depth difference upsets the curves by pivoting around a node located between the two rings (notice that in design works, this sensitivity facilitates the control rod strategy to equalize power peaks). In this case, the single channel synthesis method which assigns uniform α_i coefficients in the (x,y) plane to the $\phi_i(x,y)$ trial functions cannot correctly calculate fluxes in the radial direction.

Control rod insertion		40 cm (inner ring) 50 cm (outer ring)		40cm (inner ring) 45cm (outer ring)
Trial functions extracted from the 3D configuration - 40 cm (inner ring) - 50 cm (outer ring)		. lower blanket . follower . insertion depth diff. . absorber . upper blanket	. Follower . Absorber	. Follower . Absorber
Max. Discrepancies to reference solutions	% Keff	0.01	0.07	0.1
	% Max. Power	0.2	0.4	1.5
	% Power at the core/upper blanket boundary	1	2	8
	% Integrated power per subassembly	0.1	0.2	1
	°C Cladding temperature	0.5	1	3

TABLE I

Conclusions for design calculations

In design calculations (next section), the trial functions will be produced by 2D eigenvalue calculations representative of the core slices only. The flat and two-depression shape fluxes will be characteristic of respectively the follower and absorber (x,y) planes. The main problem arising is to know whether the trial function representative of the "ring insertion depth difference" plane can "modulate" the 3D synthesis flux in the radial direction for any movement of rod rings.

CALIBRATION OF THE SYNTHESIS METHOD FOR DESIGN CALCULATIONS

The trial functions associated to a given diluent subassembly location are produced by 2D buckled eigenvalue calculations using a single buckling applied in all groups and regions. Typical radial 2D flux distributions are presented for the characteristic planes in Figure (the core configuration investigated is given in Figures 1, 2).

1 - Table II shows the discrepancies between synthesis and reference results for several rod ring insertions and trial functions sets. One notes that in any case, a synthesis method can be calibrated to compute desired core parameters with acceptable accuracy and thereby to select start-up loadings. Figure 6 shows the error maps concerning the maximum

ponctual power and the cladding temperature per subassembly (situation of column 3, Table II). Notice also that Keff is underestimated by 0.30% ΔK/K for both "in" and "out" rod insertions : thus the control rod worth is correctly predicted. (col. 1,2, Table II).
Moreover, 3D synthesis flux used as a "guess flux" for starting a 3D finite difference calculation strongly reduces the number of outer iterations (factor 4) of the reference calculation, which confirms the validity of the synthesis results.

2 - The acceptable agreements with the reference solutions in fact hide compensated errors as shown in Figure 7. The 3D error distribution spreads changing signs around a "node" in both axial and radial directions. Below the midplane (high power zone) errors are small (max + 2%), positive in the inner core, negative in the outer core.
Above the midplane (low power zone) errors change signs abruptly (corresponding to the change of trial functions) and are increasing (to max - 20% in the inner core, + 10% in the outer core). Explanations are given in Figure 8 : in the follower and absorber slices, the synthesis fluxes have the form of the corresponding trial functions which are "asymptotical" solutions disregarding the adjacent core slices.

3 - The calibration of the trial function set changes according to the rod ring insertions :

- on one hand, the use of (O.R) trial function is absolutely advised for the state I.R < O.R (col. 4,5, Table II). Figure 9 shows its leading part concerning calculations of the maximum ponctual power, located in the "mixed trial functions" slice. For the state I.R=O.R (column 3, Table II) it does not improve the results, which is logical with the depth difference slice disappearing. Notice also that it does not in any case bring ponctual power values at core/upper blanket boundary into much better agreement.

- on the other hand, the use of (I.R) trial function is not to be recommended for the state I.R > O.R , (col. 6,7, Table II) since it increases the discrepancies as far as the maximum ponctual power is concerned. Indeed the (I.R) trial function is an "asymptotical" solution : the rise of the outer flux is exaggerated : it does not "see" the outer ring in axial direction as shown in Figure 5.

Shortly, the insertion depth difference function does not completely bring the desired effects of flux modulation in the radial direction for any movement of rod rings.

Control rod insertion inner ring (cm) outer ring (cm)		Out	In	Partially in				
		0 0	100 100	40 40	40 50		50 40	
2D calculated trial functions		Foll.	Abs.	-Foll. -Abs.	-Foll. -Abs.	-Foll. -Abs. -(OR)*	-Foll. -Abs.	-Foll. -Abs. -(IR)**
Max. discrepancies to reference solutions	Z Keff	- 0.30	- 0.30	- 0.28	- 0.35	- 0.20	- 0.25	- 0.23
	Z Max. Power	+ 0.5	+ 1.0	+ 1.0	-10.0	+ 1.0	- 0.5	- 5.0
	Z Power at the core/ upper blanket boundary	-20.0	- 3.0	-20.0	-22.0	-20.0	- 8.0	-10.0
	Z Integrated power per sub.	- 0.2	- 0.2	- 2.0	- 3.0	- 1.5	- 1.0	- 2.0
	°C Cladding temperature	- 2	- 2	- 5	- 7	- 4	- 3	- 5
TABLE II		1	2	3	4	5	6	7

*"Insertion depth difference" trial function with the absorber outer ring.
**"Insertion depth difference" trial function with the absorber inner ring.

CONCLUSION

Synthesis calculations using only two or three trial functions representative of the core slices allow to compute core parameters (Keff, maximum ponctual power, cladding temperature) with acceptable accuracy and thereby to select start-up loadings. Moreover, 3D synthesis fluxes used as "guess fluxes" for starting the 3D finite difference calculations strongly reduce the cost of reference solutions.

Yet the good agreement of some parameters must not hide the deficiencies of such a simple method. In particular, buckled eigenvalue calculations using a (x,y) region-independent buckling produce "asymptotical" solutions which disregard adjacent core slices and are too far from the "extracted" reference flux shapes.

A first improvement consists of performing 2D-HEX calculations with (x,y) region-dependent bucklings, in order to bring the effects of adjac

core slices, yet this synthesis method depends on 3D reference solutions.

Another improvement would use the multichannel synthesis, which introduces extra degrees-of-freedom into the synthesis trial function by assigning independent combining coefficients in different (x,y) regions of the plane. This method, which is independent of 3D reference solutions, has not yet be checked in the SUPER-PHENIX core design.

REFERENCES

1. C. GIACOMETTI et al, "Neutron characteristics of the SUPER-PHENIX I reactor (Creys-Malville)", International symposium on fast reactor physics, International Atomic Energy Agency, IAEA-SM-244/24, Aix-en-Provence, 24-28 September 1979.

2. S. KAPLAN, "Synthesis methods in reactor analysis", Advances in Nuclear Sciences and Technology, Vol. 3 (1966).

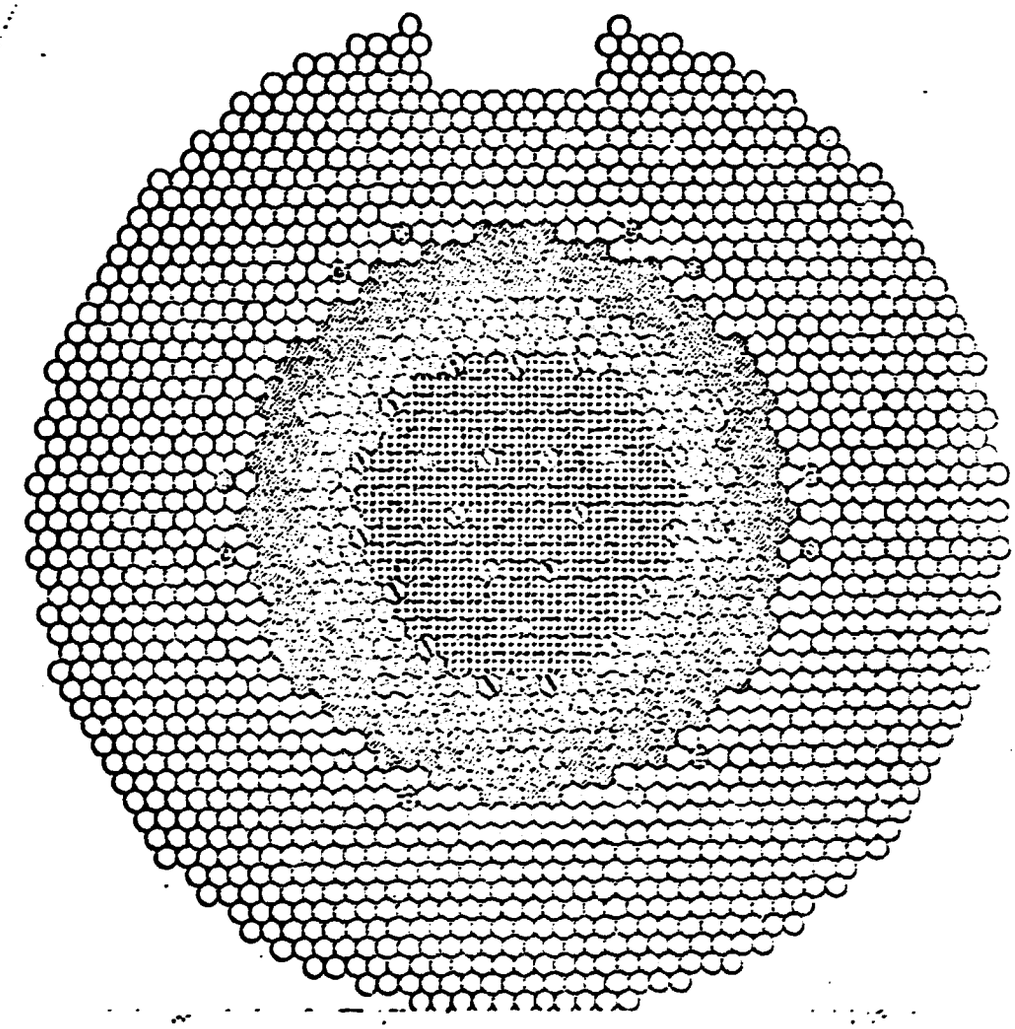

FISSILE INNER ZONE

FISSILE OUTER ZONE

DILUENT

CONTROL ROD (INNER AND OUTER RING)

BREEDER

LAYOUT OF THE SUPER-PHENIX 1 CORE

FIG 1

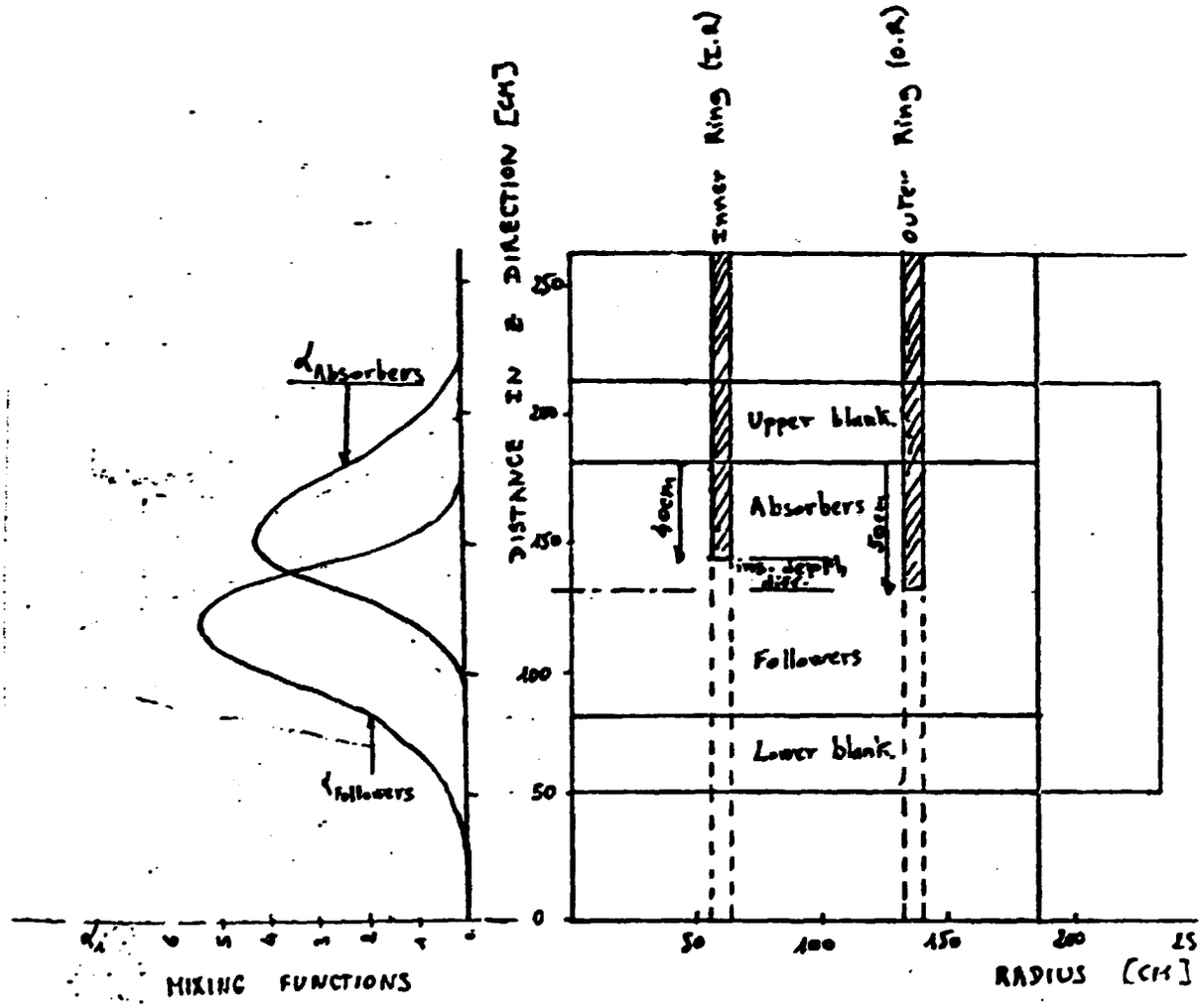

(set of two trial functions: followers and Absorbers)

LONGITUDINAL SECTION OF THE REACTOR

FIG 2

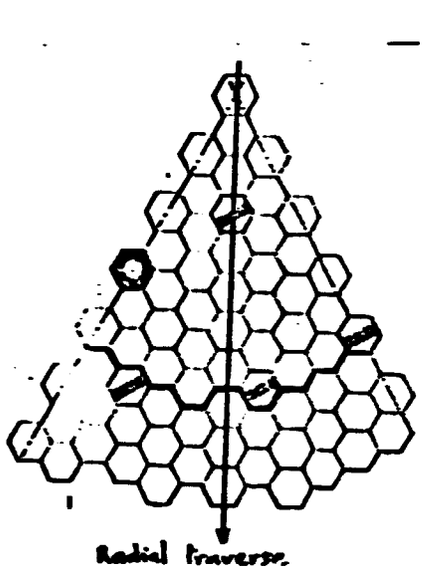

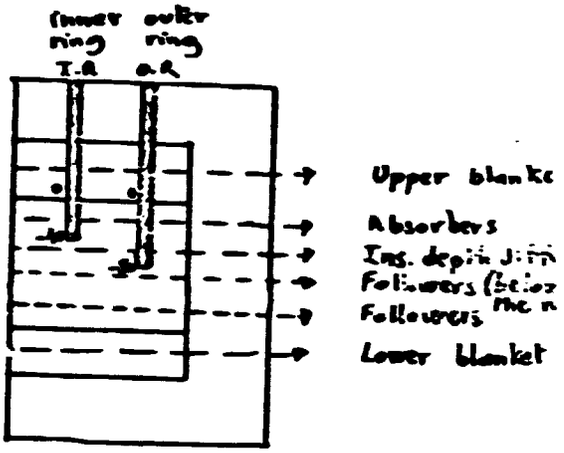

The extracted 2D-Hex fluxes are corresponding to the axial slices of the reactor

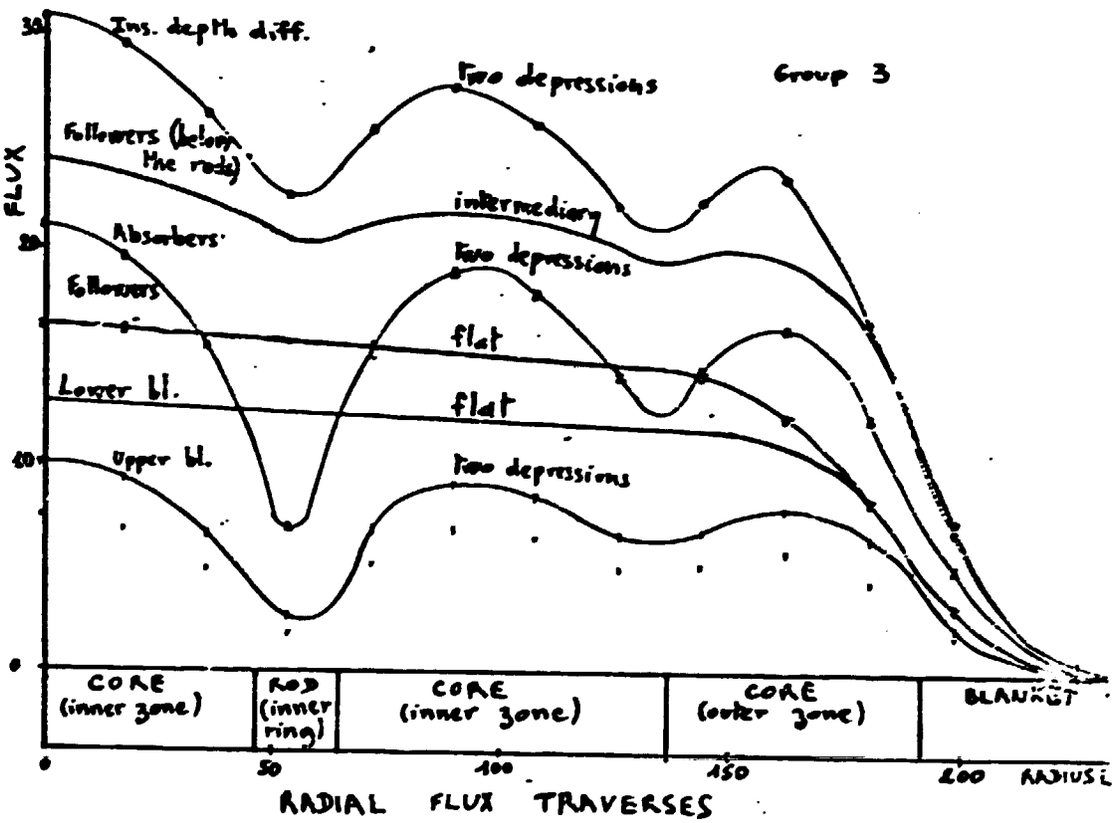

RADIAL FLUX TRAVERSES

(FROM EXTRACTED 2D-HEX TRIAL FUNCTIONS)

FIG 3

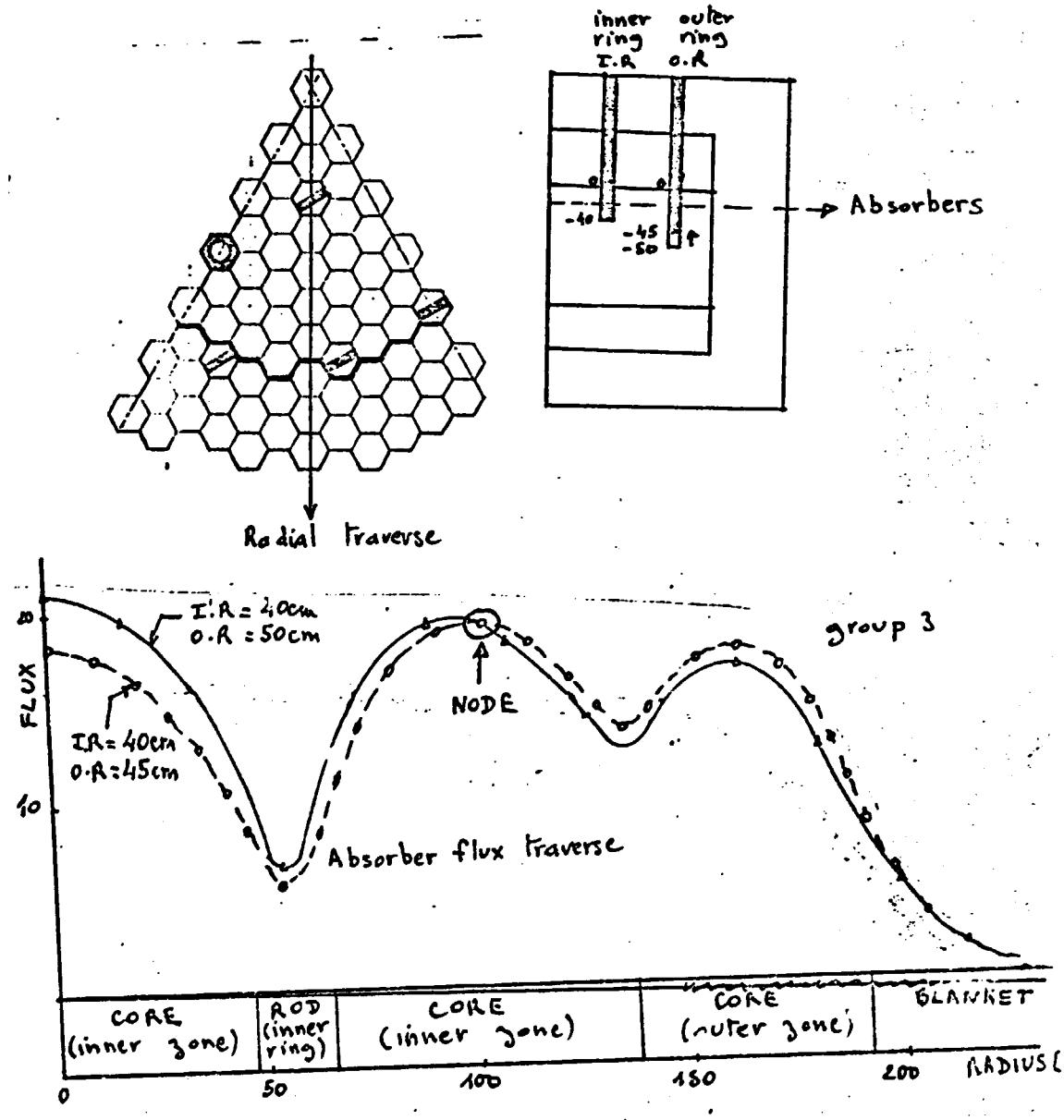

FLUX DISTURBANCES RESULTING FROM A DIFFERENTIAL MOVEMENT OF RINGS.

FIG 4

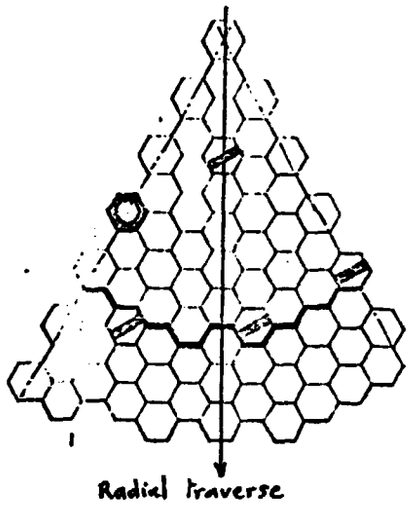

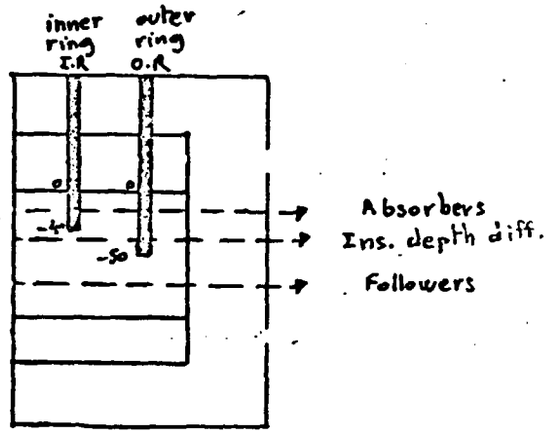

The calculated 2D-Hex fluxes are corresponding to the axial slices of the core

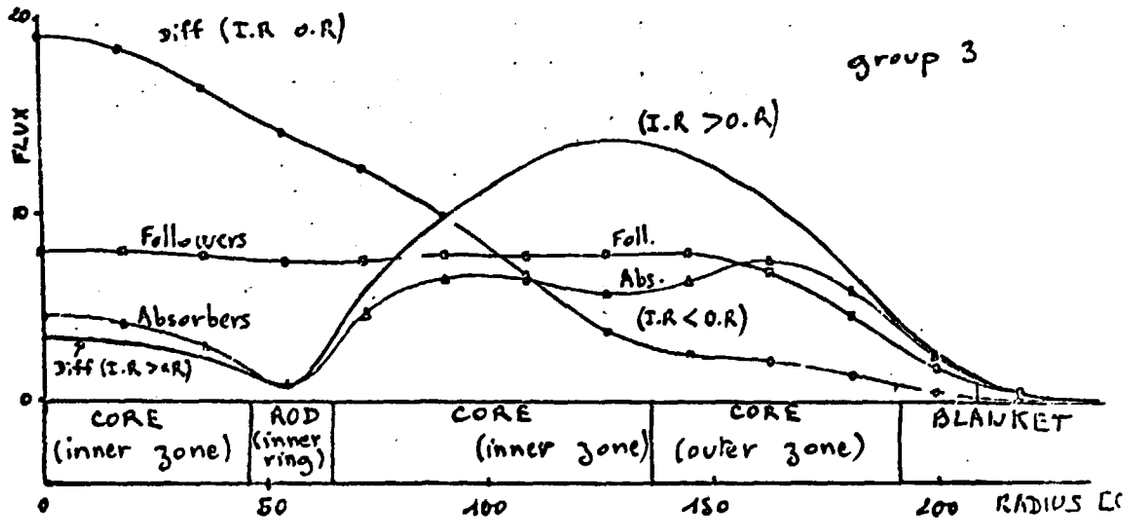

RADIAL FLUX TRAVERSES

(FROM CALCULATED 2D-HEX TRIAL FUNCTIONS

FIG 5

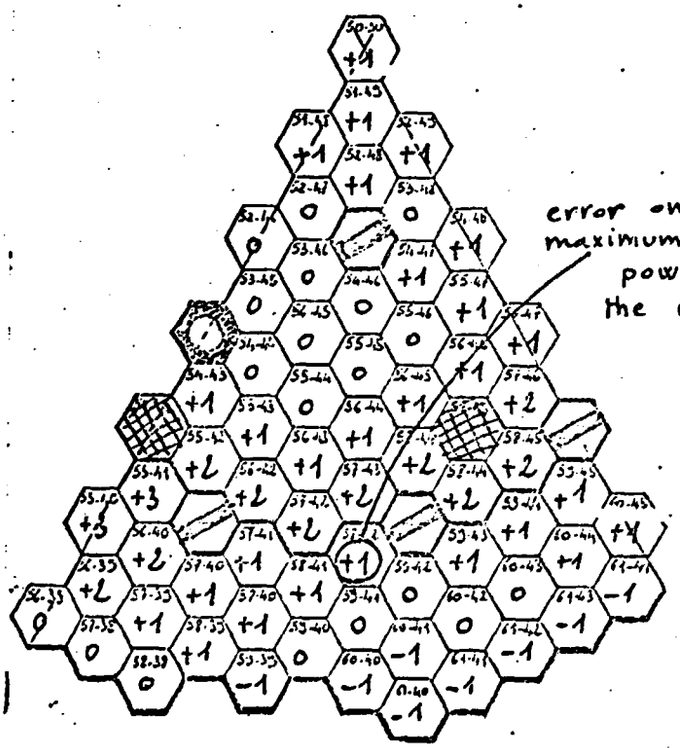

ERRORS ON MAXIMUM PONCTUAL
POWER PER SUBASSEMBLY % $\frac{\Delta P}{P}$

FIG 6

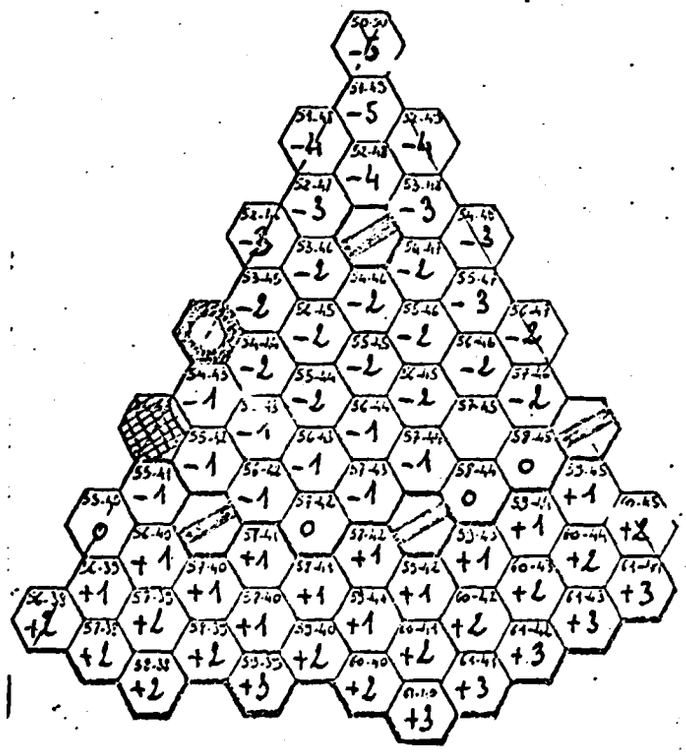

ERRORS ON CLADDING

TEMPERATURE PER SUBASSEMBLY °C ΔT

FIG 6

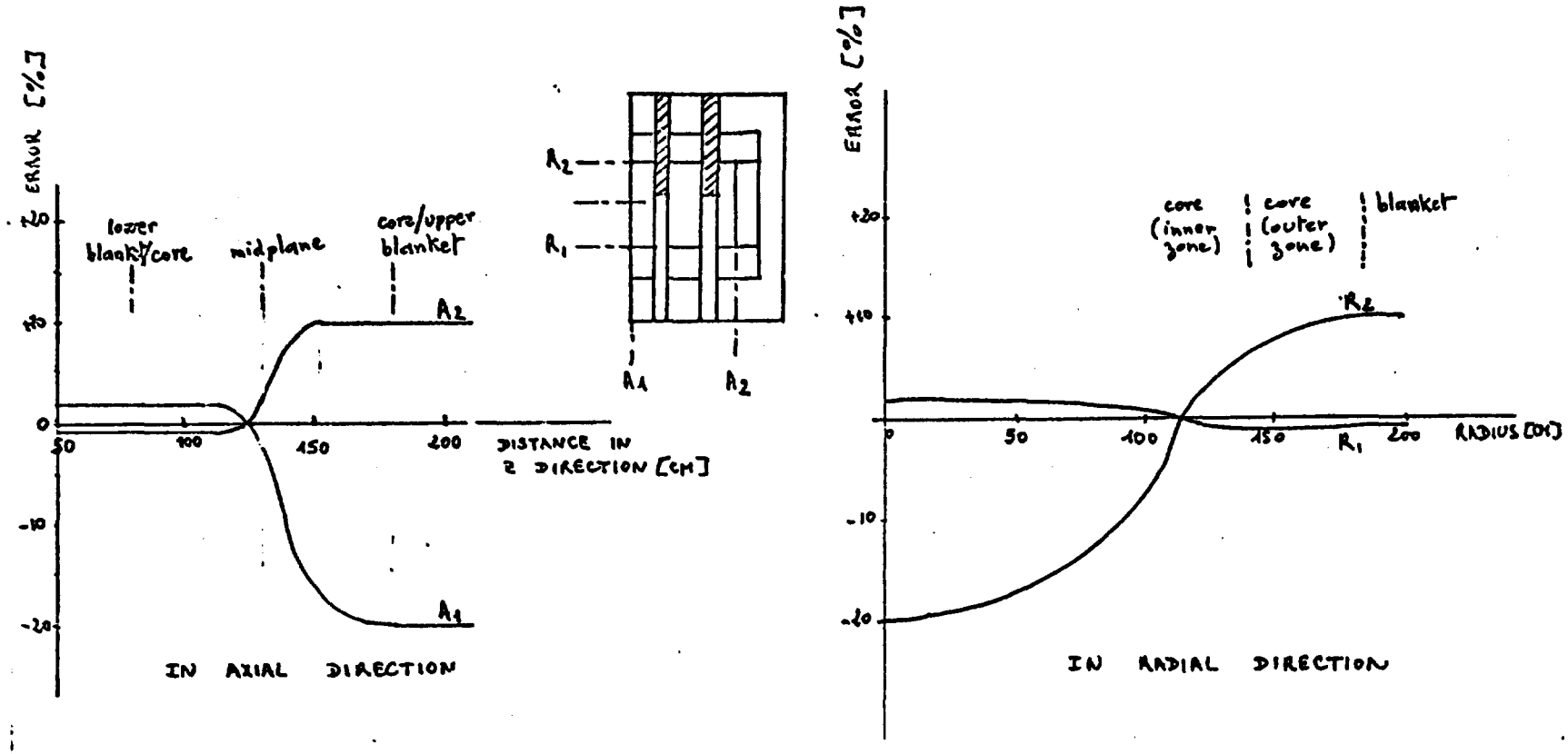

3D ERROR DISTRIBUTION ON THE PONCTUAL POWER $\left[\% \frac{\Delta P}{P} \right]$

FIG 7

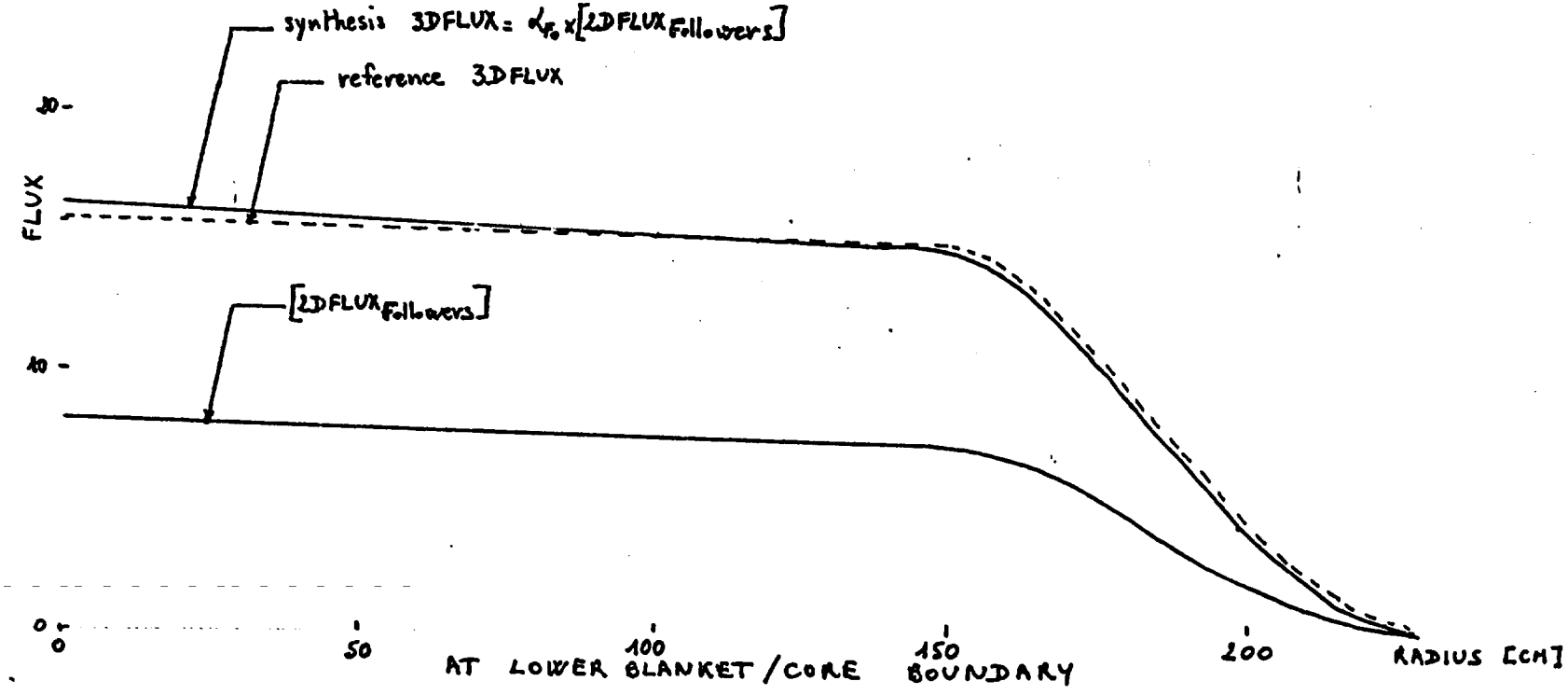

REFERENCE AND SYNTHESIS FLUX
AT CORE / AXIAL BLANKET BOUNDARIES
FIG 8

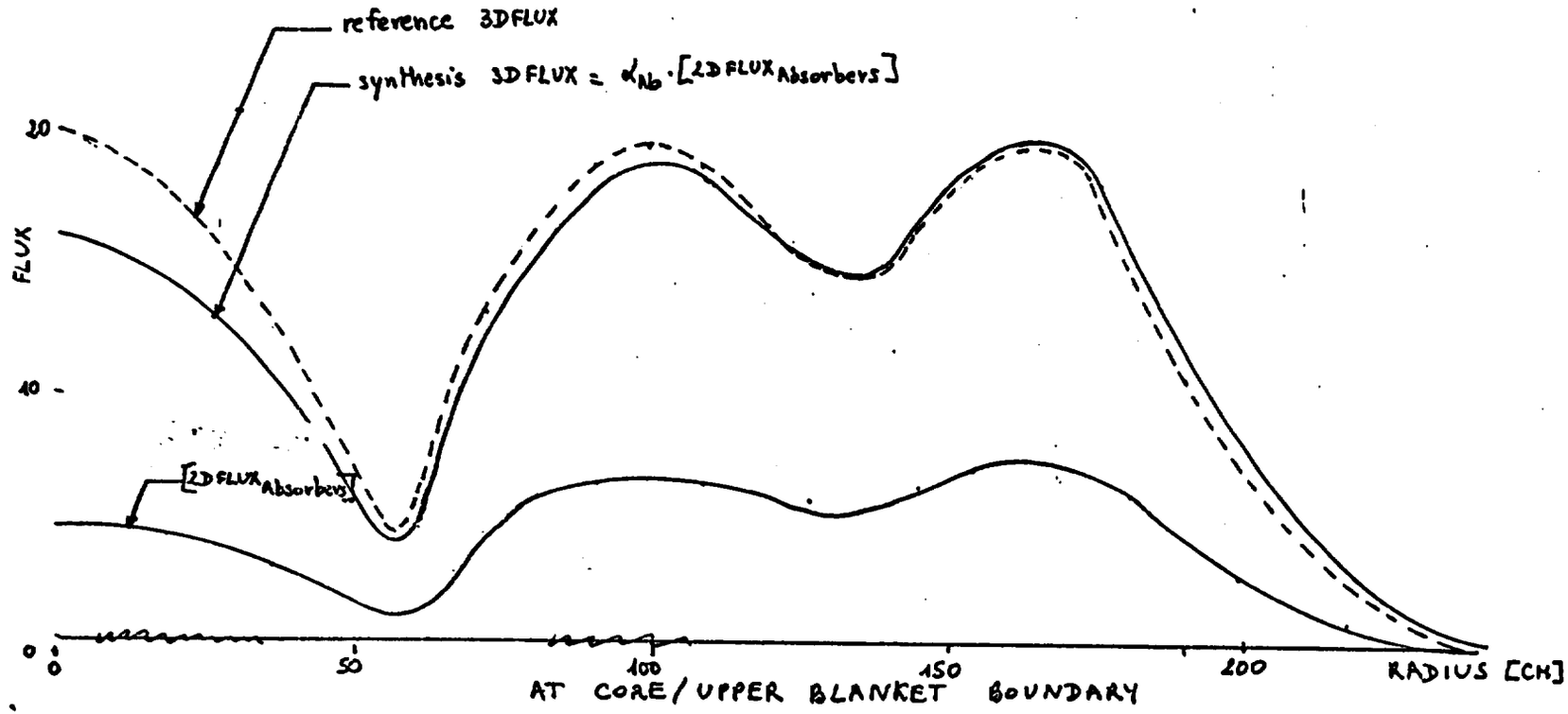
reference 3DFLUX
synthesis 3D FLUX = $\alpha_{Nb} \cdot$ [2D FLUX Absorbers]
20
40
0
FLUX
[2D FLUX Absorbers]
0
50
100
150
200
RADIUS [CM]
AT CORE/UPPER BLANKET BOUNDARY

FIG 8

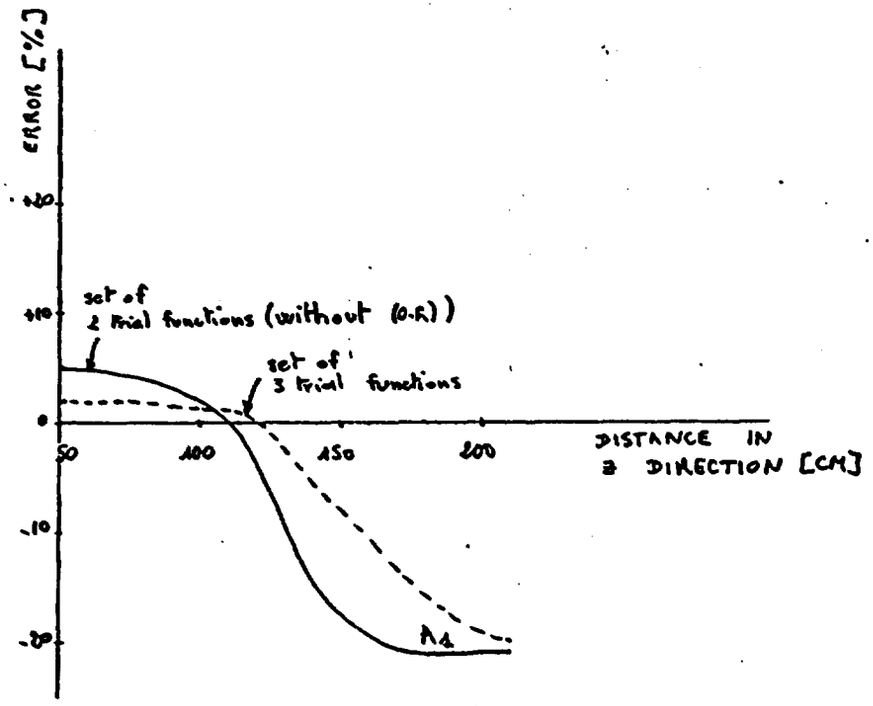

IN AXIAL DIRECTION Az
(columns 4,5, Table II)

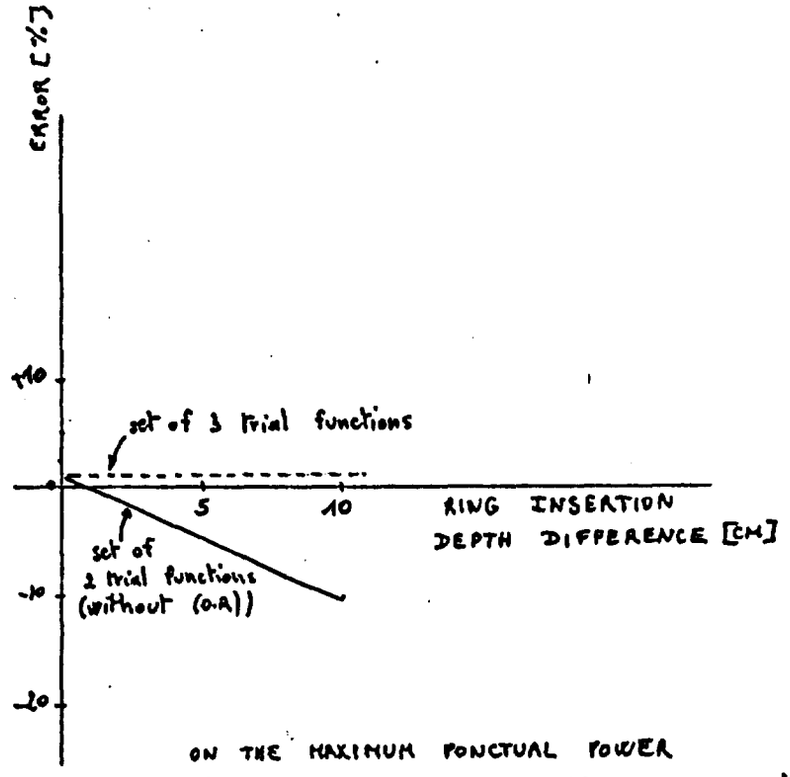

ON THE MAXIMUM PONCTUAL POWER
(for ring insertion depth differences :0-10cm)

INFLUENCE OF THE (0.A) TRIAL
FUNCTION ON THE ERROR DISTRIBUTION

FIG 9